

DYNAMIC RESPONSE OF A GUY LINE OF A GUYED TOWER TO STOCHASTIC WIND EXCITATION: 3D NON-LINEAR SMALL-SAG CABLE MODEL¹

HANNA WEBER, ANNA JABŁONKA

West Pomeranian University of Technology, Szczecin, Poland

e-mail: hanna.weber@zut.edu.pl; anna.jablonka@zut.edu.pl

RADOSŁAW IWANKIEWICZ

Calisia University, Kalisz, Poland

e-mail: r.iwankiewicz@uniwersytetkaliski.edu.pl

In the proposed approach, a 3D response of the guy line treated as a small-sag cable is considered. The strong dynamic wind action leads to the base motion excitation of the guy line. Longitudinal cable displacements are coupled with lateral ones. Hamilton's principle and Galerkin method are used to obtain the set of differential equations of motion. The cable excitation is assumed as a narrow-band stochastic process modelled as a response of an auxiliary linear filter to a Gaussian white noise process. The equivalent linearization technique is applied to obtain approximate analytical results verified against the numerical Monte Carlo simulation.

Keywords: equivalent linearization technique, non-linear system, small-sag cable, spatial response, stochastic dynamics

1. Introduction

The equations and numerical results included in this paper concern the problem presented at the 5th Polish Congress of Mechanics and 25th Conference on Computer Methods in Mechanics (PCM-CMM) which was held in September 2023. Nowadays, the use of cables in various civil engineering structures has become very popular. Classic examples include suspended or cable-stayed-bridges (Larsen and Larose, 2015). On the other hand, modern cable roof coverings are becoming more and more common (Xue *et al.*, 2022). What is worth mentioning, steel ropes are often used as flexible supports or system stabilizing elements, such as hangers (Zhu *et al.*, 2023) or guying elements in masts and towers (Shi and Salim, 2015). In each type of structures mentioned above, the function and behavior of the cable is different and requires a different approach at the design stage. Therefore, in the literature many articles dedicated to various methods of analyzing rope structures may be found, from analytical approach to complex finite element models (Ha *et al.*, 2018; Biliszczyk *et al.*, 2021).

Structural cables are flexible elements that can carry only tensile forces, however, depending on their function, types of support in the system and, above all, cross-sectional area can be considered as elements with some bending stiffness (Zhang *et al.*, 2021). It needs to be mentioned that the value of bending stiffness should be determined from experimental tests (Chen *et al.*, 2015). Due to their use in the structure, cables are exposed to external factors such as rain, snow, wind, and their slenderness makes them sensitive to various dynamic loads (Caracoglia and Zuo, 2009), which, due to randomness, should be considered using stochastic analysis (Georgakis and Taylor, 2005; Li and Chen, 2009).

¹Paper presented during PCM-CMM 2023, Gliwice, Poland

Analytical or finite element models give good results in static analysis. However, dynamics of these systems create many problems. Results from nonlinear models often differ from those obtained by experimental measurements, while complex finite element models are characterized by a large amount of time that needs to be spent on modeling and conducting the analysis. Therefore, there is a constant search for methods and tools enabling quick dynamic analysis of cables, taking into account random loads, which would support the design process.

In the presented approach, a simplified model of a single guy line in guyed towers and its 3D response to the base-motion excitation modelled as a response of an auxiliary linear filter to Gaussian white noise excitation is considered. In the guyed lines with significant length that are exposed to external factors like wind and temperature changes, most of the time some sag can be observed, even if the value of the pre-tension force is large. Therefore, the nonlinear model based on a small-sag cable is developed where longitudinal vibrations of the guyed line are coupled with transverse ones that are considered in two different directions: in and out of the cable plane. Next, the equivalent linearization technique (Socha, 2007; Roberts and Spanos, 1990) is used to solve the set of nonlinear differential equations of motion and obtain variances and cross-covariances of particular random state variables. The received results are compared with those obtained by the Monte Carlo simulation (Proppe *et al.*, 2003).

2. Nonlinear equation of motion – 3D response of a small-sag cable

In the presented approach, the initial tension in the guy line denoted as H is assumed to be very high in comparison to the effect of own weight of the rope (gravity forces), therefore the line is regarded as a small-sag cable. It is the case when the ratio of the sag to the initial length of the rope is equal or less than 1:8 (Irvine, 1981). Moreover, the 3D response of the cable is considered, where $u(x, t)$ are longitudinal displacements of the guy line, while $z(x)$ and $w(x, t)$ are the initial shape of the cable in its plane in the direction perpendicular to the guy line and the transverse displacements of the cable resulting from deformation, respectively (see Fig. 1a). The displacement out of the cable plane is denoted as $v(x, t)$ (Fig. 1b). The axial stiffness of the cable and its total length are denoted as EA and L , respectively, while mass per unit length of the rope is denoted as μ .

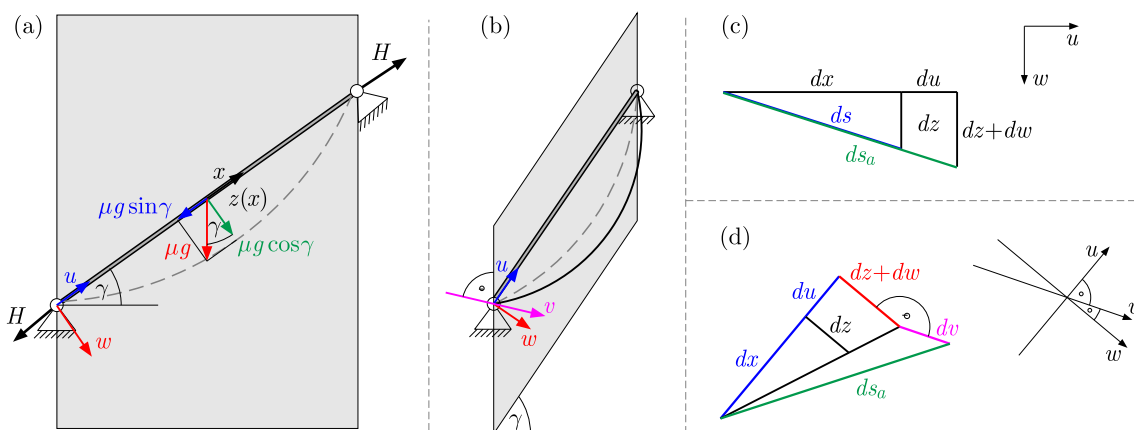


Fig. 1. Small-sag cable model of the guy line model under gravity forces: (a) planar view, (b) 3D view. Differential element of the small-sag cable: (c) planar view, (d) 3D view

If g is the gravity acceleration, the second derivative of $z(x)$ with respect to x is defined as

$$\frac{d^2 z}{dx^2} = -\frac{\mu g}{H} \cos \gamma \quad (2.1)$$

Since the small-sag cable is considered, the initial shape of the guy line can be treated as a parabola. Based on that we can assume at for the support points $z(x = 0) = 0$ and at the mid span where the maximum lateral displacement can be observed $dz/dx(x = L/2) = 0$. The integration process with using these two conditions results in the following equation

$$z = \frac{\mu g}{2H} x(L - x) \cos \gamma \tag{2.2}$$

If V and T denote the potential and kinetic energies, Hamilton's principle is given by

$$\int_0^t \delta(V - T) dt = 0 \tag{2.3}$$

For a 3D response of a cable with small sag, the kinetic energy can be expressed as

$$T = \frac{\mu}{2} \int_0^L \left(\left(\frac{\partial u}{\partial t} \right)^2 + \left(\frac{\partial w}{\partial t} \right)^2 + \left(\frac{\partial v}{\partial t} \right)^2 \right) ds \tag{2.4}$$

Using the initial shape of the cable, according to Fig. 1c, leads to

$$ds = \sqrt{dx^2 + dz^2} = \sqrt{dx^2 \left(1 + \left(\frac{dz}{dx} \right)^2 \right)} = \sqrt{1 + (z')^2} dx \tag{2.5}$$

The variation of the kinetic energy is then given by

$$\delta T = \frac{1}{2} \mu \int_0^L \delta \left(2 \frac{\partial u}{\partial t} \delta \dot{u} + 2 \frac{\partial w}{\partial t} \delta \dot{w} + 2 \frac{\partial v}{\partial t} \delta \dot{v} \right) \sqrt{1 + (z')^2} dx \tag{2.6}$$

Taking into account that the variation of the derivative equals the derivative of the variation, and assuming the vanishing of the variations δu and δw because of the fixed states at the initial time 0 and at the final time t , one obtains

$$\int_0^t \delta T = -\mu \int_0^t \int_0^L \left(\frac{\partial^2 u}{\partial t^2} \delta u + \frac{\partial^2 w}{\partial t^2} \delta w + \frac{\partial^2 v}{\partial t^2} \delta v \right) \sqrt{1 + (z')^2} dx dt \tag{2.7}$$

If $V^{(g)}$ denotes the gravitational potential energy and $N(x)$ is the cable initial static tension, the elastic potential energy of the system is given by

$$V = \underbrace{\int_0^L N(x) \varepsilon(u', w', v') ds}_{V^{(1)}} + \underbrace{\frac{EA}{2} \int_0^L \varepsilon^2(u', w', v') ds}_{V^{(2)}} + V^{(g)} \tag{2.8}$$

where ε is the normal strain defined as $\varepsilon = (ds_a - ds)/ds$, (see Fig. 1d). After neglecting the term $(\partial z/\partial x)^2$ due to its insignificant value compared to the others, the term ds_a is obtained in the following form

$$\begin{aligned} ds_a &= \sqrt{(dx + du)^2 + (dz + dw)^2 + dv^2} \\ &= dx \sqrt{1 + 2 \frac{\partial u}{\partial x} + \left(\frac{\partial u}{\partial x} \right)^2 + 2 \frac{\partial z}{\partial x} \frac{\partial w}{\partial x} + \left(\frac{\partial w}{\partial x} \right)^2 + \left(\frac{\partial v}{\partial x} \right)^2} \end{aligned} \tag{2.9}$$

If the small-sag cable is considered, the simplification $1/\sqrt{1 + (\partial z/\partial x)^2} \approx 1$ can be assumed. Using Eq. (2.4) and the Taylor series expansion results in the equation for normal strain in the presented form

$$\varepsilon \cong \frac{\partial u}{\partial x} + \frac{1}{2} \left(\frac{\partial u}{\partial x} \right)^2 + \frac{\partial z}{\partial x} \frac{\partial w}{\partial x} + \frac{1}{2} \left(\frac{\partial w}{\partial x} \right)^2 + \frac{1}{2} \left(\frac{\partial v}{\partial x} \right)^2 = u' + \frac{1}{2} (u')^2 + z' w' + \frac{1}{2} (w')^2 + \frac{1}{2} (v')^2 \tag{2.10}$$

Assuming that $N(x)/\sqrt{1+(z')^2} = H(x)$, the variation of the first term of potential energy is obtained

$$\begin{aligned}\delta V^{(1)} &= \delta \int_0^L N(x) \varepsilon(u', w', v) ds = \int_0^L N(x) \frac{\delta u' + u' \delta u' + z' \delta w' + w' \delta w' + v' \delta v'}{1+(z')^2} \sqrt{1+(z')^2} dx \\ &= \int_0^L H(x) (\delta u' + u' \delta u' + z' \delta w' + w' \delta w' + v' \delta v') dx\end{aligned}\quad (2.11)$$

Taking into account that $\delta u' = (\delta u)' = \partial \delta u / \partial x$, $\delta w' = (\delta w)' = \partial \delta w / \partial x$ and $\delta v' = (\delta v)' = \partial \delta v / \partial x$, the terms of Eq. (2.11) that depend on $u(x, t)$, $w(x, t)$ and $v(x, t)$, respectively, are defined by

$$\begin{aligned}\int_0^L H(x) (\delta u' + u' \delta u') dx &= H(x) (\delta u) \Big|_0^L - \int_0^L \frac{\partial H}{\partial x} dx \delta u + H u' \delta u \Big|_0^L - \int_0^L \frac{\partial}{\partial x} (H u') dx \delta u \\ \int_0^L H(x) (z' \delta w' + w' \delta w') dx &= H(x) z' (\delta w) \Big|_0^L - \int_0^L \frac{\partial}{\partial x} (H(x) z') dx \delta w + H(x) w' \delta w \Big|_0^L \\ &\quad - \int_0^L \frac{\partial}{\partial x} (H(x) w') dx \delta w \\ \int_0^L H(x) (v' \delta v') dx &= H(x) v' \delta v \Big|_0^L - \int_0^L \frac{\partial}{\partial x} (H(x) v') dx \delta v\end{aligned}\quad (2.12)$$

The gravitational potential energy is given by the following equation

$$V^{(g)} = - \int_0^L \mu g w ds = - \int_0^L \mu g w \sqrt{1+(z')^2} dx \quad (2.13)$$

while its variation is obtained as

$$\delta V^{(g)} = - \int_0^L \mu g \sqrt{1+(z')^2} dx \delta w \quad (2.14)$$

The below self-satisfied equation of equilibrium is subtracted from the final form of the equation of motion

$$-\frac{\partial}{\partial x} (H(x) z') - \mu g \sqrt{1+(z')^2} = 0 \quad (2.15)$$

Variation of the second term of potential energy is given by

$$\begin{aligned}\delta V^{(2)} &= \frac{EA}{2} \delta \int_0^L \varepsilon^2(u', w', v') ds = EA \int_0^L \varepsilon(u', w', v') \delta \varepsilon(u', w', v') ds \\ &\cong EA \int_0^L \left(u' + \frac{1}{2} (u')^2 + z' w' + \frac{1}{2} (w')^2 + \frac{1}{2} (v')^2 \right) (\delta u' + u' \delta u' + z' \delta w' + w' \delta w' + v' \delta v') dx\end{aligned}\quad (2.16)$$

Using the rule that the variation of the derivative is equal the derivative of the variation, particular terms of Eq. (2.16) that depend on $u(x, t)$, $w(x, t)$ and $v(x, t)$, respectively, are defined as

$$\begin{aligned}
 & EA \int_0^L \left(u' + \frac{(u')^2}{2} + z'w' + \frac{(w')^2}{2} + \frac{(v')^2}{2} \right) (1 + u') \delta u' dx \\
 &= EA \frac{\partial}{\partial x} \left[\left(u' + \frac{(u')^2}{2} + z'w' + \frac{(w')^2}{2} + \frac{(v')^2}{2} \right) (1 + u') \right] \\
 & EA \int_0^L \left(u' + \frac{(u')^2}{2} + z'w' + \frac{(w')^2}{2} + \frac{(v')^2}{2} \right) (z' + w') \delta w' dx \\
 &= EA \frac{\partial}{\partial x} \left[\left(u' + \frac{(u')^2}{2} + z'w' + \frac{(w')^2}{2} + \frac{(v')^2}{2} \right) (z' + w') \right] \\
 & EA \int_0^L \left(u' + \frac{(u')^2}{2} + z'w' + \frac{(w')^2}{2} + \frac{(v')^2}{2} \right) (v') \delta v' dx \\
 &= EA \frac{\partial}{\partial x} \left[\left(u' + \frac{(u')^2}{2} + z'w' + \frac{(w')^2}{2} + \frac{(v')^2}{2} \right) (v') \right]
 \end{aligned} \tag{2.17}$$

If Hamilton's principle is used (Eq. (2.3)) for Eqs. (2.12) and Eqs. (2.17), the following set of equations is obtained

$$\begin{aligned}
 & -\frac{\partial}{\partial x} (H(x)u') - EA \frac{\partial}{\partial x} \left[\left(u' + \frac{(u')^2}{2} + z'w' + \frac{(w')^2}{2} + \frac{(v')^2}{2} \right) (1 + u') \right] + \mu \frac{\partial^2 u}{\partial t^2} = 0 \\
 & -\frac{\partial}{\partial x} (H(x)w') - EA \frac{\partial}{\partial x} \left[\left(u' + \frac{(u')^2}{2} + z'w' + \frac{(w')^2}{2} + \frac{(v')^2}{2} \right) (z' + w') \right] + \mu \frac{\partial^2 w}{\partial t^2} = 0 \\
 & -\frac{\partial}{\partial x} (H(x)v') - EA \frac{\partial}{\partial x} \left[\left(u' + \frac{(u')^2}{2} + z'w' + \frac{(w')^2}{2} + \frac{(v')^2}{2} \right) (v') \right] + \mu \frac{\partial^2 v}{\partial t^2} = 0
 \end{aligned} \tag{2.18}$$

3. Base motion excitation – dynamics of a guy line

The displacement $U(t)$ of a tower at the point of attachment of the guy line is treated as a base motion excitation for guy line vibration (see Fig. 2). For the case that the horizontal displacement of the guyed tower is out the cable plane, the components $U_u(t) = U(t) \cos \gamma \cos \eta$ and $U_w(t) = U(t) \sin \gamma \cos \eta$, are

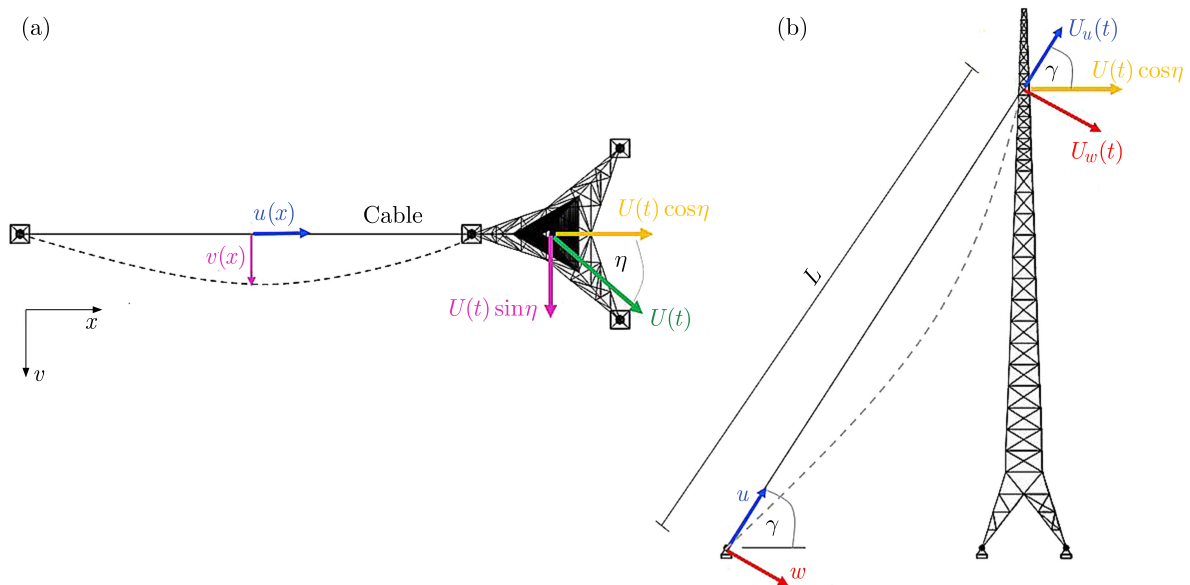


Fig. 2. Guy line base motion: (a) top view, (b) in cable plane view

excitations for motion in the longitudinal and transverse direction in the cable plane, respectively, while $U_v(t) = U(t) \sin \eta$ is the base motion excitation in the out of plane direction, where γ and η are the slope of the cable and the angle in the horizontal plane between the direction of displacements $U(t)$ and cable plane, respectively. If $\bar{u}(x, t)$, $\bar{w}(x, t)$ and $\bar{v}(x, t)$ denote absolute motions expressed in terms of the relative motions $u(x, t)$, $w(x, t)$ and $v(x, t)$, which are related with elastic deformations and base motion due to $U(t)$, they can be given by

$$\begin{aligned}\bar{u}(x, t) &= \frac{x}{L}U(t) \cos \gamma \cos \eta + u(x, t) & \bar{w}(x, t) &= \frac{x}{L}U(t) \sin \gamma \cos \eta + w(x, t) \\ \bar{v}(x, t) &= \frac{x}{L}U(t) \sin \eta + v(x, t)\end{aligned}\quad (3.1)$$

Equation (2.18) expressed by absolute motions is obtained as

$$\begin{aligned}& \int_0^L \left\{ -\frac{\partial H(x)}{\partial x} \frac{\partial \bar{u}}{\partial x} - H(x) \frac{\partial^2 \bar{u}}{\partial x^2} - EA \frac{\partial}{\partial x} \left[\frac{\partial \bar{u}}{\partial x} + \frac{3}{2} \left(\frac{\partial \bar{u}}{\partial x} \right)^2 + \frac{\partial z}{\partial x} \frac{\partial \bar{w}}{\partial x} + \frac{1}{2} \left(\frac{\partial \bar{w}}{\partial x} \right)^2 \right. \right. \\ & \quad \left. \left. + \frac{1}{2} \left(\frac{\partial \bar{v}}{\partial x} \right)^2 + \frac{1}{2} \left(\frac{\partial \bar{u}}{\partial x} \right)^3 + \frac{\partial \bar{u}}{\partial x} \frac{\partial z}{\partial x} \frac{\partial \bar{w}}{\partial x} + \frac{1}{2} \frac{\partial \bar{u}}{\partial x} \left(\frac{\partial \bar{w}}{\partial x} \right)^2 + \frac{1}{2} \frac{\partial \bar{u}}{\partial x} \left(\frac{\partial \bar{v}}{\partial x} \right)^2 \right] + \mu \frac{\partial^2 \bar{u}}{\partial t^2} \right\} \delta \bar{u} \, dx \\ & + \int_0^L \left\{ -\frac{\partial H(x)}{\partial x} \frac{\partial \bar{w}}{\partial x} - H(x) \frac{\partial^2 \bar{w}}{\partial x^2} - EA \frac{\partial}{\partial x} \left[\frac{\partial \bar{u}}{\partial x} \frac{\partial z}{\partial x} + \frac{1}{2} \left(\frac{\partial \bar{u}}{\partial x} \right)^2 \frac{\partial z}{\partial x} + \left(\frac{\partial z}{\partial x} \right)^2 \frac{\partial \bar{w}}{\partial x} \right. \right. \\ & \quad \left. \left. + \frac{3}{2} \frac{\partial z}{\partial x} \left(\frac{\partial \bar{w}}{\partial x} \right)^2 + \frac{1}{2} \left(\frac{\partial \bar{v}}{\partial x} \right)^2 \frac{\partial z}{\partial x} + \frac{\partial \bar{u}}{\partial x} \frac{\partial \bar{w}}{\partial x} + \frac{1}{2} \left(\frac{\partial \bar{u}}{\partial x} \right)^2 \frac{\partial \bar{w}}{\partial x} + \frac{1}{2} \left(\frac{\partial \bar{w}}{\partial x} \right)^3 \right. \right. \\ & \quad \left. \left. + \frac{1}{2} \left(\frac{\partial \bar{v}}{\partial x} \right)^2 \frac{\partial \bar{w}}{\partial x} \right] + \mu \frac{\partial^2 \bar{w}}{\partial t^2} \right\} \delta \bar{w} \, dx + \int_0^L \left\{ -\frac{\partial H(x)}{\partial x} \frac{\partial \bar{v}}{\partial x} - H(x) \frac{\partial^2 \bar{v}}{\partial x^2} \right. \\ & \quad \left. - EA \frac{\partial}{\partial x} \left[\frac{\partial \bar{u}}{\partial x} \frac{\partial \bar{v}}{\partial x} + \frac{1}{2} \left(\frac{\partial \bar{u}}{\partial x} \right)^2 \frac{\partial \bar{v}}{\partial x} + \frac{\partial z}{\partial x} \frac{\partial \bar{w}}{\partial x} \frac{\partial \bar{v}}{\partial x} + \frac{1}{2} \left(\frac{\partial \bar{w}}{\partial x} \right)^2 \frac{\partial \bar{v}}{\partial x} + \frac{1}{2} \left(\frac{\partial \bar{v}}{\partial x} \right)^3 \right] + \mu \frac{\partial^2 \bar{v}}{\partial t^2} \right\} \delta \bar{v} \, dx = 0\end{aligned}\quad (3.2)$$

Using the relationships $\delta \bar{u}(x, t) = \delta u(x, t)$, $\delta \bar{w}(x, t) = \delta w(x, t)$ and $\delta \bar{v}(x, t) = \delta v(x, t)$, the time derivatives are expressed by

$$\begin{aligned}\frac{\partial^2 \bar{u}}{\partial t^2} &= \frac{x}{L} \ddot{U}(t) \cos \gamma \cos \eta + \frac{\partial^2 u}{\partial t^2} & \frac{\partial^2 \bar{w}}{\partial t^2} &= \frac{x}{L} \ddot{U}(t) \sin \gamma \cos \eta + \frac{\partial^2 w}{\partial t^2} \\ \frac{\partial^2 \bar{v}}{\partial t^2} &= \frac{x}{L} \ddot{U}(t) \sin \eta + \frac{\partial^2 v}{\partial t^2}\end{aligned}\quad (3.3)$$

When the derivatives with respect to x are considered, the base motion terms vanish. Using Galerkin's method and single-mode approximation, the particular displacements are defined as

$$u(x, t) = p(t) \sin \frac{\pi x}{L} \quad w(x, t) = q(t) \sin \frac{\pi x}{L} \quad v(x, t) = r(t) \sin \frac{\pi x}{L} \quad (3.4)$$

and, consequently, their variations are given by

$$\delta u(x, t) = \delta p(t) \sin \frac{\pi x}{L} \quad \delta w(x, t) = \delta q(t) \sin \frac{\pi x}{L} \quad \delta v(x, t) = \delta r(t) \sin \frac{\pi x}{L} \quad (3.5)$$

In the considered small-sag cable model, the initial tension is much more significant in comparison to the dead load of the line, therefore $H = \text{const}$ can be assumed. After including damping forces depending on relative velocities $-c_u \partial u / \partial t$, $-c_w \partial w / \partial t$ and $-c_v \partial v / \partial t$ together with Eqs. (3.3)-(3.5) in Eq. (3.2), and after integration, the following set of nonlinear equations is obtained

$$\begin{aligned}\ddot{p}(t) + a_1 p(t) + a_2 p^3(t) - 2a_3 p(t)q(t) + a_2 p(t)q^2(t) + a_2 p(t)r^2(t) + \frac{c_u}{\mu} \dot{p}(t) + Ha_1 p(t) &= -\beta_u \ddot{U}(t) \\ \ddot{q}(t) - a_3 p^2(t) - a_4 q(t) - 3a_3 q^2(t) - a_3 r^2(t) + a_2 p^2(t)q(t) + a_2 q^3(t) + a_2 r^2(t)q(t) & \\ + \frac{c_w}{\mu} \dot{q}(t) + Ha_1 q(t) &= -\beta_w \ddot{U}(t) \\ \ddot{r}(t) + a_2 p^2(t)r(t) - 2a_3 q(t)r(t) + a_2 q^2(t)r(t) + a_2 r^3(t) + \frac{c_v}{\mu} \dot{r}(t) + Ha_1 r(t) &= -\beta_v \ddot{U}(t)\end{aligned}\quad (3.6)$$

where the particular constant terms are denoted as

$$\begin{aligned} a_1 &= \frac{\pi^2}{\mu L^2} & a_2 &= EA \frac{3\pi^4}{8\mu L^4} & a_3 &= -EA \frac{14g\pi}{9HL^2} \cos \gamma \\ a_4 &= -EA \left(\frac{\mu g}{H} \cos \gamma \right)^2 \left(\frac{6 + \pi^2}{12\mu} \right) & \beta_u &= \frac{2}{\pi} \cos \gamma \cos \eta \\ \beta_w &= \frac{2}{\pi} \sin \gamma \cos \eta & \beta_v &= \frac{2}{\pi} \sin \eta \end{aligned}$$

4. Stochastic governing equations

The structure displacement $U(t)$ is assumed to be dominated by the fundamental mode shape of the tower with the corresponding natural frequency Ω_o . Since the stochastic wind excitation in the form of a strong wind gust can be treated as a stationary wide band process, the process $U(t)$ is considered as a narrow-band one, with the central frequency Ω_o . In the presented approach, it is assumed as the Gaussian white noise passed through the first-order linear filter, giving the process $X(t)$, which is subsequently passed through the second-order linear filter. Therefore, the process $U(t)$ is governed by the stochastic equations defined as

$$\ddot{U} + 2\zeta_f \Omega_o \dot{U} + \Omega_o^2 U = X(t) \quad \dot{X} + \alpha X = \alpha \sqrt{2\pi S_o} \xi(t) \quad (4.1)$$

where ζ_f is damping of the linear filter, $\xi(t)$ denotes a Gaussian white noise while S_o is its spectral density. It should be noted that the process $U(t)$, as the displacement response, must be twice differentiable. That condition will be fulfilled if

$$\int_{-\infty}^{\infty} \omega^4 S_{UU}(\omega) d\omega < \infty \quad \text{where} \quad S_{UU}(\omega) = \frac{S_o \alpha^2}{(\omega^2 + \alpha^2)[(\Omega_o^2 - \omega^2)^2 + (2\zeta_f \Omega_o \omega)^2]} \quad (4.2)$$

$S_{UU}(\omega)$ is the spectral density of the process $U(t)$ while its steady-state variance σ_U^2 is given by the following expression

$$\sigma_U^2 = \frac{\alpha \pi S_o (2\zeta_f \Omega_o + \alpha)}{2\zeta_f \Omega_o^3 (2\alpha \zeta_f \Omega_o + \alpha^2 + \Omega_o^2)} \quad \text{with} \quad \alpha = \Omega_o \left(-\zeta_f + \sqrt{\zeta_f^2 + \frac{\zeta_f \Omega_o^3 A_0^2}{\pi S_o - \zeta_f \Omega_o^3 A_0^2}} \right) \quad (4.3)$$

The expression for α is obtained from the condition of the mean-square equivalence of the horizontal displacement response $U(t)$ to the harmonic process with the amplitude A_0 , frequency Ω_o and variance $\sigma_U^2 = A_0^2/2$. Using Eqs. (3.6) together with Eqs. (4.1) leads to the set of differential equations of motion

$$\begin{aligned} \ddot{p}(t) &= -a_1(EA + H)p(t) - a_2 p^3(t) + 2a_3 p(t)q(t) - a_2 p(t)q^2(t) - a_2 p(t)r^2(t) - \frac{c_u}{\mu} \dot{p}(t) - \beta_u \ddot{U}(t) \\ \ddot{q}(t) &= a_3 p^2(t) + a_4 q(t) + 3a_3 q^2(t) + a_3 r^2(t) - a_2 p^2(t)q(t) - a_2 q^3(t) - a_2 r^2(t)q(t) \\ &\quad - \frac{c_w}{\mu} \dot{q}(t) - a_1 H q(t) - \beta_w \ddot{U}(t) \\ \ddot{r}(t) &= -a_2 p^2(t)r(t) + 2a_3 q(t)r(t) - a_2 q^2(t)r(t) - a_2 r^3(t) - \frac{c_v}{\mu} \dot{r}(t) - a_1 H r(t) - \beta_v \ddot{U}(t) \\ \ddot{U}(t) &= X(t) - 2\zeta_f \Omega_o \dot{U}(t) - \Omega_o^2 U(t) \quad \dot{X} = -\alpha X + \alpha \sqrt{2\pi S_o} \xi(t) \end{aligned} \quad (4.4)$$

The stochastic equations of motion in state space form are

$$\dot{\mathbf{Y}}(t) = \mathbf{c}(\mathbf{Y}(t))dt + \boldsymbol{\sigma}dW(t) \quad (4.5)$$

where $W(t)$ denotes the standard Wiener process, $\mathbf{c}(\mathbf{Y}(t))$ is the drift vector and $\boldsymbol{\sigma}$ means the diffusion vector. If the state vector is assumed as $\mathbf{Y}(t) = [p(t), \dot{p}(t), q(t), \dot{q}(t), r(t), \dot{r}(t), U(t), \dot{U}(t), X(t)]^T$, the particular elements of the drift vector are obtained as

$$\begin{aligned}
c_1(\mathbf{Y}(t)) &= \dot{p}(t) \\
c_2(\mathbf{Y}(t)) &= -a_1(EA + H)p(t) - a_2p^3(t) + 2a_3p(t)q(t) - a_2p(t)q^2(t) - a_2p(t)r^2(t) - \frac{c_u}{\mu}\dot{p}(t) \\
&\quad + \beta_u(\Omega_o^2U(t) + 2\zeta_f\Omega_o\dot{U}(t) - X(t)) \\
c_3(\mathbf{Y}(t)) &= \dot{q}(t) \\
c_4(\mathbf{Y}(t)) &= a_3p^2(t) + a_4q(t) + 3a_3q^2(t) + a_3r^2(t) - a_2p^2(t)q(t) - a_2q^3(t) - a_2r^2(t)q(t) \\
&\quad - \frac{c_w}{\mu}\dot{q}(t) - a_1Hq(t) + \beta_w(\Omega_o^2U(t) + 2\zeta_f\Omega_o\dot{U}(t) - X(t)) \\
c_5(\mathbf{Y}(t)) &= \dot{r}(t) \\
c_6(\mathbf{Y}(t)) &= -a_2p^2(t)r(t) + 2a_3q(t)r(t) - a_2q^2(t)r(t) - a_2r^3(t) - \frac{c_v}{\mu}\dot{r}(t) - a_1Hr(t) \\
&\quad + \beta_v(\Omega_o^2U(t) + 2\zeta_f\Omega_o\dot{U}(t) - X(t)) \\
c_7(\mathbf{Y}(t)) &= \dot{U}(t) \\
c_8(\mathbf{Y}(t)) &= -\Omega_o^2U(t) - 2\zeta_f\Omega_o\dot{U}(t) + X(t) \\
c_9(\mathbf{Y}(t)) &= -\alpha X(t)
\end{aligned} \tag{4.6}$$

and the diffusion vector is defined as

$$\boldsymbol{\sigma} = [0, 0, 0, 0, 0, 0, 0, 0, \alpha\sqrt{2\pi S_o}]^T \tag{4.7}$$

5. Equivalent (statistical) linearization approach

The augmented state vector transformation to the centralized state vector is required to convert the original nonlinear set of differential equations into the linear one by using the equivalent linearization technique (ELT). The centralized state vector is defined as

$$\mathbf{Y}^0(t) = [Y_1^0, Y_2^0, Y_3^0, Y_4^0, Y_5^0, Y_6^0, Y_7^0, Y_8^0, Y_9^0]^T \tag{5.1}$$

where its particular elements are given by $Y_i^0(t) = Y_i(t) - E[Y_i(t)]$. The stochastic equation expressed in terms of the centralized state vector $\mathbf{Y}^0(t)$ and centralized drift vector $\mathbf{c}^0(\mathbf{Y}^0(t), t)$ is defined as

$$d\mathbf{Y}^0(t) = \mathbf{c}^0(\mathbf{Y}^0(t), t)dt + \boldsymbol{\sigma}(t)dW(t) \tag{5.2}$$

with

$$\mathbf{c}^0(\mathbf{Y}^0(t), t) = \mathbf{c}(\mathbf{Y}^0(t), t) - E[\mathbf{c}(\mathbf{Y}^0(t), t)]$$

The idea of the equivalent linearization technique is the replacement of the original non-linear equation given by Eq. (4.5) with a linear one defined as

$$d\mathbf{Y}^0(t) = \mathbf{B}\mathbf{Y}^0(t)dt + \boldsymbol{\sigma}dW(t) \tag{5.3}$$

where the centralized drift terms are expressed by the linear function of the state variables $\mathbf{Y}^0(t)$ and equivalent coefficients \mathbf{B} . Using the condition of minimization of mean-square errors between the original model and the linear one, the equivalent coefficients can be determined from the following expression

$$B_{im}\kappa_{mj} = E[Y_j^0 c_i^0(\mathbf{Y}^0)] \tag{5.4}$$

where κ_{mj} denotes the covariance function of the state variables m and j . The centralized state variables \mathbf{Y}^0 are jointly Gaussian distributed, therefore in further consideration, the relationship given by Atalik Utku (1976) is used

$$E[\mathbf{X}f(\mathbf{X})] = E[\mathbf{X}\mathbf{X}^T]E[\nabla f(\mathbf{X})] \tag{5.5}$$

where \mathbf{X} is the zero-mean Gaussian random vector, $f(\mathbf{X})$ denotes a non-linear function and ∇ is given by the following expression $\nabla = [\partial/\partial X_1, \partial/\partial X_2, \dots, \partial/\partial X_n]^T$. If Eq. (5.5) is used in transposed form of Eq. (5.4), the following expression is obtained

$$\boldsymbol{\kappa}(t)\mathbf{B}^T = \boldsymbol{\kappa}(t)E[\nabla \mathbf{c}^{0T}(\mathbf{Y}^0(t))] \quad \text{with} \quad \mathbf{B}^T = E[\nabla \mathbf{c}^{0T}(\mathbf{Y}^0(t))] \tag{5.6}$$

The result of applying Eq. (5.6) to the elements of the centralized drift vector is the matrix \mathbf{B} defined as

$$\mathbf{B} = \begin{bmatrix} 0 & 1 & 0 & 0 & 0 & 0 & 0 & 0 & 0 \\ b_1 & -\frac{c_u}{\mu} & b_2 & 0 & b_3 & 0 & \beta_u \Omega_o^2 & 2\beta_u \zeta_f \Omega_o & -\beta_u \\ 0 & 0 & 0 & 1 & 0 & 0 & 0 & 0 & 0 \\ b_2 & 0 & b_4 & -\frac{c_w}{\mu} & b_5 & 0 & \beta_w \Omega_o^2 & 2\beta_w \zeta_f \Omega_o & -\beta_w \\ 0 & 0 & 0 & 0 & 0 & 1 & 0 & 0 & 0 \\ b_3 & 0 & b_5 & 0 & b_6 & -\frac{c_v}{\mu} & \beta_v \Omega_o^2 & 2\beta_v \zeta_f \Omega_o & -\beta_v \\ 0 & 0 & 0 & 0 & 0 & 0 & 0 & 1 & 0 \\ 0 & 0 & 0 & 0 & 0 & 0 & -\Omega_o^2 & -2\zeta_f \Omega_o & 1 \\ 0 & 0 & 0 & 0 & 0 & 0 & 0 & 0 & -\alpha \end{bmatrix}$$

where

$$\begin{aligned} b_1 &= -a_1(EA + H) - a_2 \left(3E[(Y_1^0)^2] + 3(E[p(t)])^2 \right) + E[(Y_3^0)^2] + (E[q(t)])^2 + E[(Y_5^0)^2] \\ &\quad + (E[r(t)])^2 + 2a_3 E[q(t)] \\ b_2 &= -2a_2(E[Y_1^0 Y_3^0] + E[q(t)]E[p(t)]) + 2a_3 E[p(t)] \\ b_3 &= -2a_2(E[Y_1^0 Y_5^0] + E[r(t)]E[p(t)]) \\ b_4 &= -a_2 \left(E[(Y_1^0)^2] + (E[p(t)])^2 + 3E[(Y_3^0)^2] + 3(E[q(t)])^2 + E[(Y_5^0)^2] + (E[r(t)])^2 \right) \\ &\quad + 6a_3 E[q(t)] + a_4 - a_1 H \\ b_5 &= -2a_2 \left(E[Y_5^0 Y_3^0] + E[r(t)]E[q(t)] \right) + 2a_3 E[r(t)] \\ b_6 &= -a_1 H - a_2 \left(3E[(Y_5^0)^2] + 3(E[r(t)])^2 + E[(Y_1^0)^2] + (E[p(t)])^2 + E[(Y_3^0)^2] + (E[q(t)])^2 \right) \\ &\quad + 2a_3 E[q(t)] \end{aligned}$$

To obtain variances and covariances of particular random state variables, the following set of differential equations for the covariance matrix $\kappa_{\mathbf{Y}^0 \mathbf{Y}^0} = E[\mathbf{Y}^0 \mathbf{Y}^{0T}]$ should be solved

$$\frac{d}{dt} \kappa_{\mathbf{Y}^0 \mathbf{Y}^0} = \mathbf{B} \kappa_{\mathbf{Y}^0 \mathbf{Y}^0} + \kappa_{\mathbf{Y}^0 \mathbf{Y}^0} \mathbf{B}^T + \sigma \sigma^T \quad (5.7)$$

together with the differential equations for mean values defined by

$$\frac{d}{dt} E[\mathbf{Y}(t)] = E[\mathbf{c}(\mathbf{Y}^0(t), t)] \quad (5.8)$$

As a result, a set of 54 differential equations is obtained that can be solved numerically.

6. Numerical examples – results and discussion

In the considered problem, the simplified model of a steel guyed tower with a single guy line is examined. The tower with triangular cross-section supported on three pin supports that is presented in Fig. 2 was firstly considered by the finite element method (FEM). The total height of the structure is assumed as 300 m while the point at which the guy line is attached to the tower is located on the level 252 m. The slope of the cable is assumed as $\gamma = 57^\circ$, that gives the total length of the guy line equal to $L = 300$ m. The mass-per unit length of the steel rope and its longitudinal stiffness are assumed as $\mu = 7.47$ kg/m and $EA = 195$ MN, respectively. In the FEM analysis, the particular bars are modeled as 3D beam elements while the guy line as an elastic cable with a given pre-tension. It turns out that the presence of the guy line in the model does not affect the result of the whole system fundamental frequency, that equals $\Omega_0 = 1.82$ rad/s, which corresponds to the assumption that the cable has no significant influence on the fundamental frequency of the tower. However the static analysis of the guyed tower under the dead load of structural elements and static wind load gives a conclusion that the value of the pre-tension force has influence on the maximum horizontal displacement of the guy line attachment point. It turns out that the higher the value of the pretension force the larger the horizontal displacement in the structure. It is

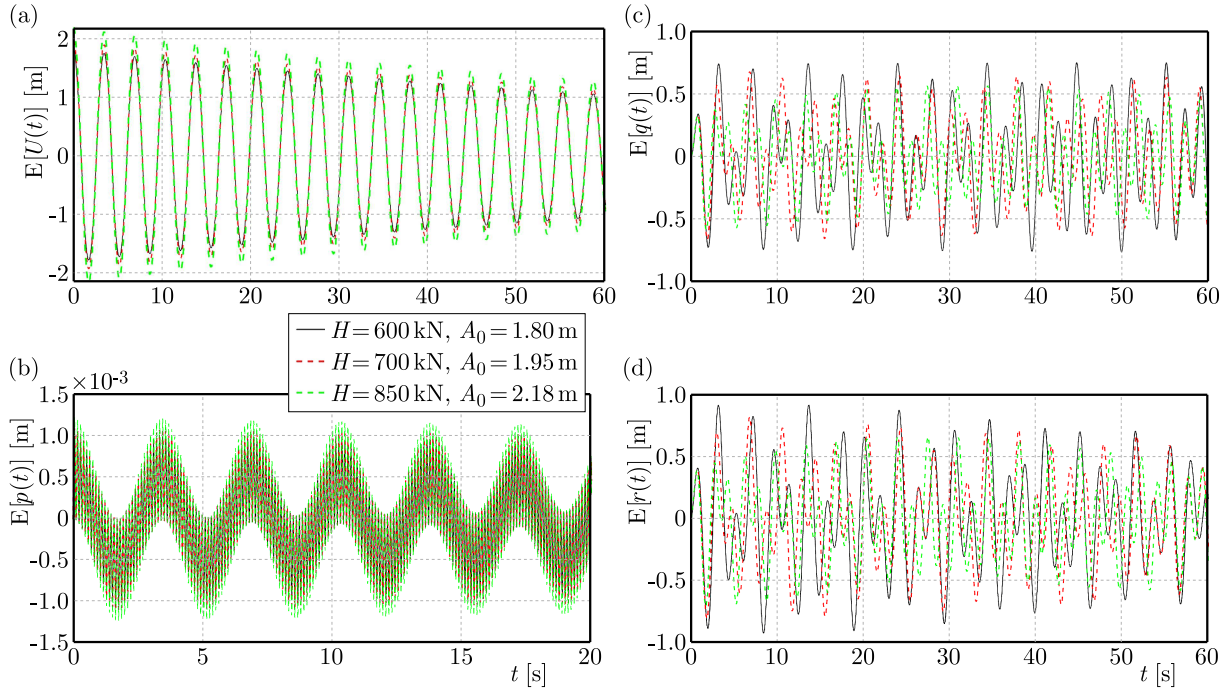


Fig. 3. Expected values of particular random state variables for various initial tension obtained by ELT

observed when the wind acts on the tower in the opposite direction to the action of the cable, it makes the rope compressed, so it is inactive, but its initial tension leads to an increase in displacement.

The maximum value of the tower horizontal displacement under the static load obtained by the FEM method is taken as the amplitude A_0 of the process $U(t)$ together with the corresponding pre-tension force H in the presented nonlinear model, Eqs. (5.7) and (5.8). The results of expected values obtained by the equivalent linearization technique (ELT) for selected cases are presented in Fig. 3. In every case, the Gaussian white noise process spectral density, damping of the linear filter and damping coefficients are assumed as $S_0 = 1$, $\zeta_f = 0.005$ and $c_u = c_w = c_v = 0.03 \text{ Ns/m}^2$, respectively. It is considered that the wind is acting parallel to the cable plane, therefore $\eta = 0^\circ$ is assumed. The whole motion is examined during 60 s, however for clarity of presentation, some results with significant vibration frequency are presented in a shorter time interval. As it can be seen, the bigger the amplitude A_0 , the larger the expected values of the tower horizontal displacement $E[U(t)]$ (Fig. 3a) and the expected generalized coordinate of cable longitudinal vibrations $E[p(t)]$ (Fig. 3b), which seems natural. It is worth noticing that even if the wind is acting parallel to the cable plane, the results of expected values of generalized coordinates of the cable lateral vibrations in and out of the plane, i.e. $E[q(t)]$ (Fig. 3c) and $E[r(t)]$ (Fig. 3d), respectively, are comparable. However, the behaviour of these random variables is opposite to the longitudinal displacement. Increasing the pre-tension force, which leads to increasing its stiffness due to the greater axial force, results in decreasing the expected values of generalized coordinate in the cable lateral vibration.

The same regularity can be observed in diagrams of the variances of particular random state variables. In the case of $\text{Var}[X(t)]$ (Fig. 4a), $\text{Var}[U(t)]$ (Fig. 4b) and $\text{Var}[p(t)]$ (Fig. 4c) increasing the amplitude of the tower horizontal displacement leads to increasing the value of the variance. On the other hand, the lower pre-tension force leads to decreasing the stiffness of the guy line and, consequently, the variances of generalized coordinates of cable lateral vibration in and out of the guy line plane increase (compare Fig. 4d,e), but they are also comparable.

However, for the lowest values of the initial tension some wrong negative results of the variance of velocity of the longitudinal cable vibrations $\text{Var}[\dot{p}(t)]$ are obtained (not reported here in the figure). All results of expected values and variances of particular random state variables are obtained directly from numerical solution of the differential set of equations described by Eqs. (5.7) and (5.8). As is well known, no variance can be negative. Such behaviour may be caused by numerical errors that arise in the solution of the set of differential equations because of very small final results. On the other hand, it should be also admitted that the ELT method has some limitations, namely when non-linearity of the considered

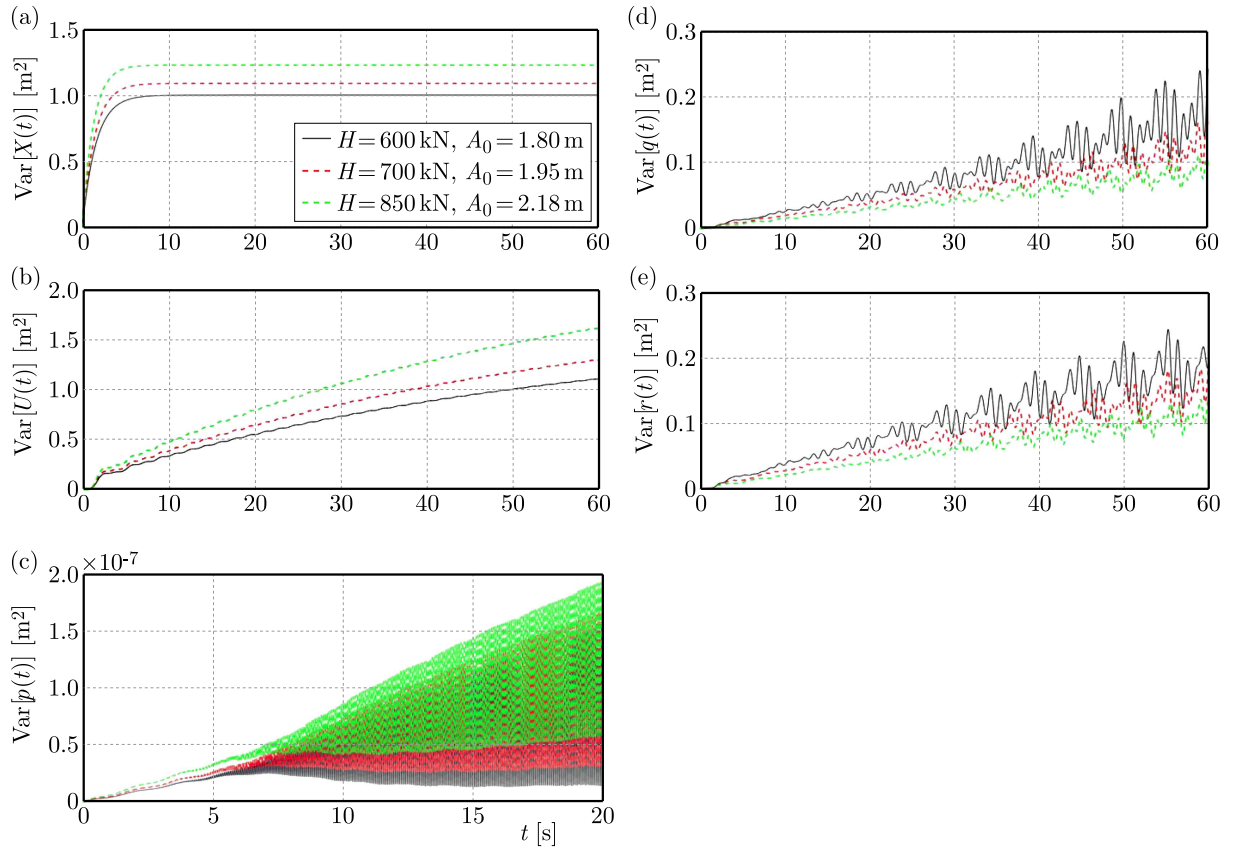


Fig. 4. Variances of particular random state variables for various initial tension

problem is strong, it can result in the incorrect results. Therefore, some additional numerical tests were conducted and the comparison of the course of variances $\text{Var}[\dot{p}(t)]$ obtained for different directions of wind action, $H = 850$ kN and $A_0 = 2.18$ m were made. During the wind action in the cable plane ($\eta = 0^\circ$), the results of variance are positive, but when the action of the wind is changed to $\eta = 45^\circ$ and the other parameters of motion remain unchanged, the non-linearities arise and some results become negative. This confirmed the previous assumption.

The obtained results were verified by the Monte Carlo Simulation (MCS) conducted for the set of equations (4.4) with using 4000 sample functions and time step of computations $\Delta t = 0.005$ s. The value of standard deviation of the Gaussian white noise process simulated in the numerical computations is adopted as $1/\sqrt{\Delta t}$ (Weber *et al.*, 2021), to obtain results independent of the time step. Due to the very long time needed to conduct the simulation, only first 20 s of motion were examined. The comparison of diagrams obtained by both methods for $H = 850$ kN, $A_0 = 2.18$ m, $S_0 = 1$ and $\zeta_f = 0.005$ are presented in Figs. 5-6. As it can be seen, the expected values and variances of particular random state variables obtained from ELT and MCS are in good agreement. Only in the case of variance of the longitudinal cable vibration $\text{Var}[\dot{p}(t)]$ the results from ELT show a bigger amplitude of vibration in comparison to the results from the MCS. However, the MCS diagram course is exactly in the middle of that obtained by the ELT and additionally the meaningful values are very small, so the difference may be caused by numerical errors. The main advantage of the ELT method is easy application in numerical calculation and a very short time needed to obtain the result in comparison to the MCS, which takes many hours due to the large number of sample functions required to get smooth diagrams.

7. Concluding remarks

The presented approach shows that the nonlinear 3D response of the cable in the considered model of the guyed tower under stochastic excitation can be successfully solved by using an equivalent linearization technique. As it is shown, the obtained results are comparable with those obtained by the Monte Carlo

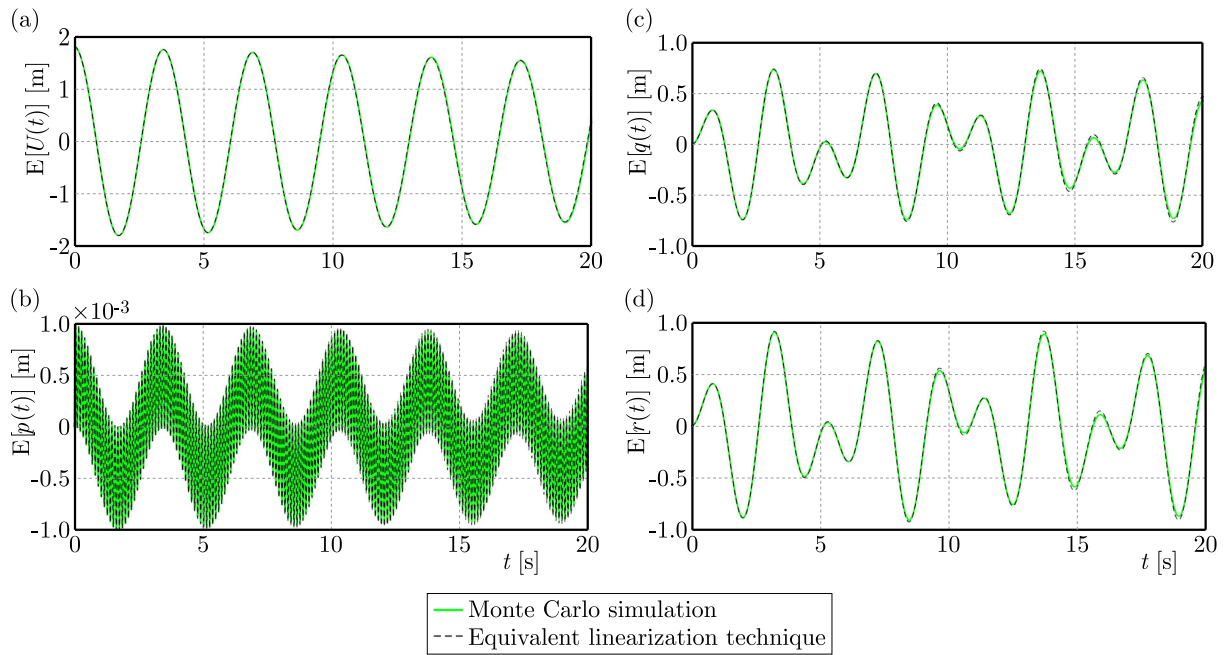


Fig. 5. Comparison of expected values of particular random state variables

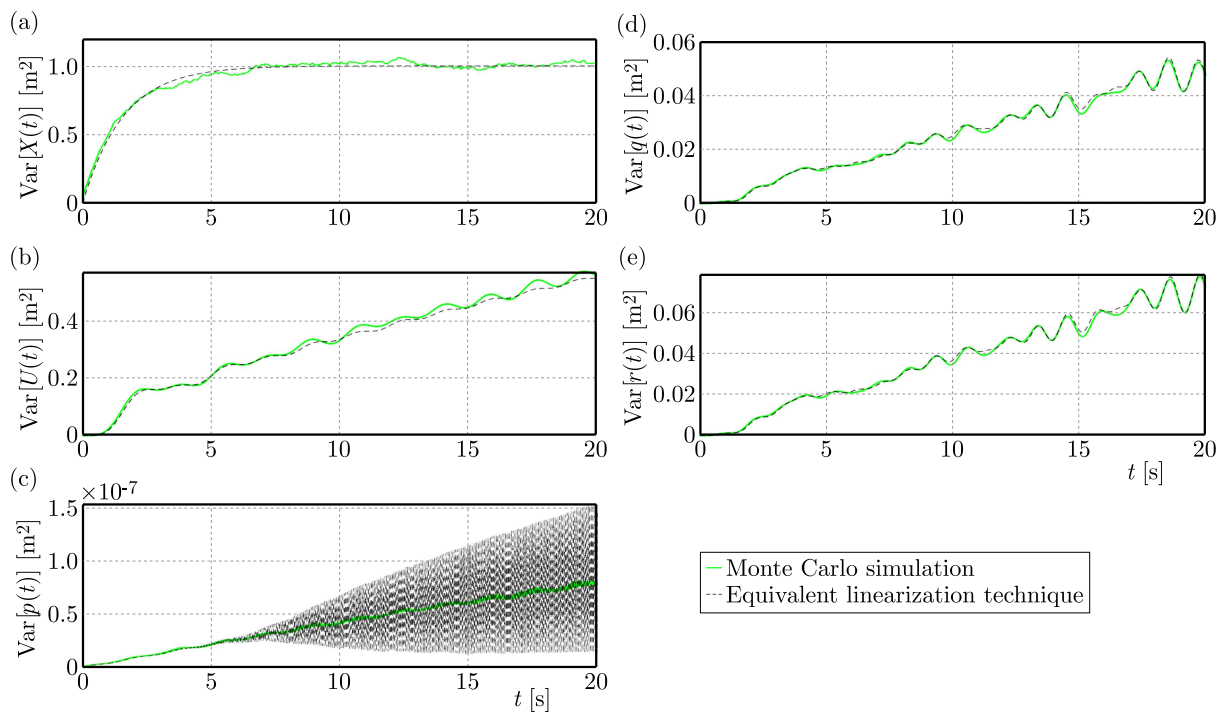


Fig. 6. Comparison of variances of particular random state variables

simulation and, furthermore, the time needed to conduct nonlinear analysis is significantly shorter. This fact together with easy application of this approach in numerical computations presents the opportunity to create a tool that can be very useful at the stage of designing structures with guy lines. A small-sag cable model more closely corresponds to the actual behaviour of the guy line in comparison to an elastic string. Additionally its 3D response under the wind excitation in various direction gives a possibility for deeper examination of the problem of random vibrations in cable systems.

References

1. ATALIK T.S., UTKU S., 1976, Stochastic linearization of multi-degree-of-freedom nonlinear systems, *Earthquake Engineering Structures Dynamics*, **4**, 411-420
2. BILISZCZUK J., HAWRYSZKÓW P., TEICHGRAEBER M., 2021, SHM system and a FEM model-based force analysis assessment in stay cables, *Sensors*, **21**, 6, 1927
3. CARACOGLIA L., ZUO D., 2009, Effectiveness of cable networks of various configurations in suppressing stay-cable vibration, *Engineering Structures*, **31**, 12, 2851-2864
4. CHEN Z., YU Y., WANG X., WU X., LIU H., 2015, Experimental research on bending performance of structural cable, *Construction and Building Materials*, **96**, 279-288
5. GEORGAKIS C.T., TAYLOR C.A., 2005, Nonlinear dynamics of cable stays. Part 2: Stochastic cable support excitation, *Journal of Sound and Vibration*, **281**, 3-5, 565-591
6. HA M.-H., VU Q.-A., TRUONG V.-H., 2018, Optimum design of stay cables of steel cable-stayed bridges using nonlinear inelastic analysis and genetic algorithm, *Structures*, **16**, 288-302
7. IRVINE H.M., 1981, *Cable Structures*, The MIT Press, Cambridge, Massachusetts and London
8. LARSEN A., LAROSE G.L., 2015, Dynamic wind effects on suspension and cable-stayed bridges, *Journal of Sound and Vibration*, **334**, 2-28
9. LI J., CHEN J., 2009, *Stochastic Dynamics of Structures*, John Wiley & Sons
10. PROPPE C., PRADLWARTER H.J., SCHÜELLER G.I., 2003, Equivalent linearization and Monte Carlo simulation in stochastic dynamics, *Probabilistic Engineering Mechanics*, **18**, 1, 1-15
11. ROBERTS J.B., SPANOS P.D., 1990, *Random Vibration and Statistical Linearization*, John Wiley and Sons, New York
12. SOCHA L., 2007, *Linearization Methods for Stochastic Dynamic Systems*, Springer, Berlin Heidelberg
13. SHI H., SALIM H., 2015, Geometric nonlinear static and dynamic analysis of guyed towers using fully nonlinear element formulations, *Engineering Structures*, **99**, 492-501
14. WEBER H., KACZMARCZYK R., IWANKIEWICZ R., 2021, Non-linear response of cable-mass-spring system in high-rise buildings under stochastic seismic excitation, *Materials*, **14**, 22, 6858
15. XUE S., LI X., LIU Y., 2022, Advanced form finding of cable roof structures integral with supporting frames: Numerical methods and case studies, *Journal of Building Engineering*, **60**, 105204
16. ZHANG W., LU X., WANG Z., LIU Z., 2021, Effect of the main cable bending stiffness on flexural and torsional vibrations of suspension bridges: Analytical approach, *Engineering Structures*, **240**, 112393
17. ZHU L., CHEN T., CHEN L., LU Z., HU X., HUANG X., 2023, Experimental testing and residual performance evaluation of existing hangers with steel pipe protection taken from an in-service tied-arch bridge, *Applied Sciences*, **13**, 19, 11070